



OPEN Effects of nano-berberine and berberine loaded on green synthesized selenium nanoparticles on cryopreservation and in vitro fertilization of goat sperm

Mehrangiz Piri¹, Amir Hossein Mahdavi^{1✉}, Mehdi Hajian^{2✉},
Mohammad Hossein Nasr-Esfahani², Leila Soltani³ & Nima Tanhaei Vash²

After cryopreservation, reactive oxygen species (ROS) can damage sperm. Antioxidants are the primary defense against oxidative damage. Berberine is a bioactive alkaloid found in *Berberis vulgaris*, *Curcuma longa*, and *Ergon grape*, and is a potent antioxidant. Due to the negative effects of free radicals in oxidative stress processes, antioxidant chemicals are required to protect sperm. However, berberine has low bioavailability, making it less effective. Loading techniques on nanoparticles and nanotechnology can help overcome this limitation. Selenium nanoparticles were synthesized with barberry extract, and berberine was loaded on them. Berberine nanoparticles were then synthesized using anti-solvent precipitation with a syringe pump technique. The synthesis of nanoparticles was confirmed by EDX, UV-visible, FE-SEM, Zeta-Potential, and FTIR tests. In this experiment, we aim to investigate the impact of nano-berberine and berberine loaded on Se-NPs on goat sperm parameters after freeze-thawing. We assessed the generation of reactive oxygen species (ROS), in vitro fertility, and the subsequent embryo development of zygote with treated sperm after determining the optimal concentration of various chemicals on sperm parameters. The study found that all treatments had significant differences from the control group in terms of motility, viability, DNA and membrane integrity, ROS level, lipid peroxidation, in vitro fertility ability, and the capacity to develop inseminated oocytes ($p < 0.05$). The most significant outcomes were observed with berberine loaded on Se-NPs and the combination of selenium nanoparticles with berberine nanoparticles.

Keywords Berberine loaded on Se-NPs, Nano-berberine, Goat, Embryo, Sperm cryopreservation

Artificial insemination (AI) is the oldest biotechnological method with roots dating back to the 18th century. It is a fundamental technology and an essential aid for modern methods in animal breeding¹. Preservation of spermatozoa requires specific steps to avoid premature aging, including reducing sperm metabolism, depleting ATP, and preventing the production of detrimental byproducts including reactive oxygen species (ROS) by using chemical inhibitors or lowering the temperature². When the production of free oxygen radicals increases, it leads to oxidative stress. ROS is generated by mammalian spermatozoa and is associated with defective sperm function. The imbalance between ROS and sperm antioxidant activity is the main cause of the cryo-damage of sperm³. Antioxidants are molecules that dispose of, scavenge, and inhibit the formation of ROS or oppose their actions⁴.

Berberine (Br) is an isoquinoline alkaloid found in the stem bark and roots of *Berberis aristata* (family Berberidaceae), commonly known as “Daru haldi” in Urdu. Br formulations are widely used in Ayurveda and traditional Chinese medicine to treat hypertension and inflammatory conditions⁵. However, the poor water solubility of Br affects its dissolution rate and bioavailability, limiting its clinical use⁶. With a log P-value of -1.5 , Br is classified as a class III drug in the biopharmaceutical classification system (BCS). Drugs in this class

¹Department of Animal Science, College of Agriculture, Isfahan University of Technology, Isfahan, Iran. ²Department of Animal Biotechnology, Reproductive Biomedicine Research Center, Royan Institute for Biotechnology, ACECR, Isfahan, Iran. ³Department of Animal Sciences, Faculty of Agriculture and Natural Resources, Razi University, Kermanshah, Iran. ✉email: mahdavi@iut.ac.ir; mehdihajian2002@gmail.com

are lipophobic, have poor membrane permeability, and their absorption is mainly limited to the paracellular pathway⁷. This leads to low bioavailability due to malabsorption of the drug and its first-pass effect in the intestine, with the absolute bioavailability of Br in rats being less than 1%⁸.

There have been various methods utilized to tackle the issues of reduced bioavailability and poor solubility. To enhance solubility, some of the techniques that have been employed include particle size reduction, solid dispersion, and the use of drug nanoparticles (NPs). NPs are smaller in size than typical drug particles, which results in an increased surface area for the drug⁹.

Nanotechnology is a powerful technology that has the potential to benefit the livestock industry, particularly through the manipulation of semen used in artificial insemination¹⁰. Nanoparticles have unique chemical, physical, and biological properties that have attracted scientific interest over the past few decades. However, their use in industries such as food science and cosmetics is limited due to concerns about their potential effects on the environment and bioaccumulation¹¹. Nanoparticles with a diameter of 1–100 nanometers have shown promising results for improving fertility in different animal species¹². Nano-elements have low toxicity and high bioavailability because they exhibit novel characteristics, such as more specific surface area, numerous active surface centers, high surface activity, high catalytic efficiency, and strong adsorption ability¹³.

Nanobiotechnology shows the merging of nanotechnology and biotechnology to develop a green, synthetic, and eco-friendly technology for the synthesis of nanomaterials¹⁴. The nanoparticles synthesized through the green method are found to be non-toxic, cost-effective, and biodegradable in nature¹⁵. The green method of synthesizing nanoparticles utilizes natural materials such as fruits, flowers, roots, and microorganisms like bacteria, algae, and fungi¹⁵.

Numerous methods have been employed to address the issues of poor solubility and reduced bioavailability when it comes to medications. These findings are significant because they could potentially reduce the amount of medication required to treat illnesses¹⁶.

Certain studies have demonstrated that Selenium (Se) supplementation can have a protective effect during the storage and incubation of sperm in animal models^{17,18}. Se nanoparticles (Se-NPs) are less toxic than sodium selenite¹⁹. Additionally, various clinical and experimental studies have investigated the impact of Se-NPs administration on semen quality in goat buck²⁰, rats²¹, bull¹⁹, and in vitro in roosters²².

This study aimed to synthesize berberine nanoparticles and load them onto green selenium nanoparticles synthesized with barberry extract. The study focuses on the specific properties of these nanoparticles. Additionally, there is a lack of information regarding the effects of nano-berberine and berberine loaded on Se-NPs as an antioxidant on the quality of cryopreserved spermatozoa of goats. Therefore, this study aims to investigate the effect of nano-berberine and berberine loaded on Se-NPs on cryopreservation and in vitro fertilization in goat sperm. An eco-friendly approach will be employed by using aqueous extracts of *Berberis vulgaris* fruit.

Results

The results of making nanoparticles

Energy-dispersive X-ray analysis (EDX)

The synthesized nanoparticles were analyzed for their chemical elemental composition using EDX. In the case of Br-NPs, EDX analysis showed four signals: a high signal from the C atom (79.78%), signals from the O atom (16.36%), Cl atom (3.01%), and N atom (0.84%). Other elements did not have any peaks (Fig. 1A). The analysis revealed the existence of prominent peaks from Se atoms at 1.0–2.0 keV and additional faint signals of O and C for all nanoparticles connected to the samples' organic molecules. The EDX analysis of Se-NPs revealed five signals: a high signal from the Se atom (57.72%), signals from the O atom (36.23%), C atom (4.98%), N atom (1.03%), and Cl atom (0.04%). Other elements did not show any peaks (Fig. 1B). Furthermore, the EDX spectra of Br loaded on Se-NPs showed four signals: a significant signal from the Se atom (59.49%), as well as signals from the C atom (35.55%), O atom (4.95%), and Cl atom (0.02%). Other elements did not have any peaks (Fig. 1C).

Ultraviolet-visible (UV-visible) absorption spectrum

The absorption spectra of Se-NPs and Br-co-SeNPs synthesized through a green process were examined to determine the loading of Br on Se-NPs. The spectra were obtained by adding dried SeNPs and Br-co-SeNPs to a solution and then using double-distilled water to determine the absorbance after ultrasonic stirring for 10 min. The conjugation was found to be effective as the maximum wavelength shifted from 294 to 370 nm, an increase of around 76 nm. The quantity of medication combined with the synthesized Se-NPs was measured using a UV-visible spectrophotometer. The unconjugated drug was separated by centrifugation to calculate the conjugation efficiency using the standard curve equation: $y = 0.5935x + 0.0947$. The results showed that the conjugation efficiency was approximately 42.25% (supplementary Fig. 1).

Field emission scanning electron microscopy (FE-SEM) analysis

FE-SEM can be used to study the surface topography of nanomaterials and determine their potential applications. Br-NPs, as observed in FE-SEM images, had a consistent rectangular shape and were less than 100 nm in size (Fig. 2A). The morphology of Se-NP is shown in Fig. 2B, and the results suggest the presence of clumps of nanoparticles that resemble porous structures. Spherical nanoparticles have a unique optical absorption peak of 1.5 keV due to surface plasmon resonance. Figure 2 shows the size of the synthesized nanoparticles and FE-SEM images.

Zeta-potential

In supplementary Fig. 2A, a distinct peak at 0 mV (of $\geq \pm 25$ mV) is visible for the synthesized Br-NPs. To achieve stable dispersions, it is recommended to have a zeta potential of $\geq \pm 25$ mV. This is because repulsive forces

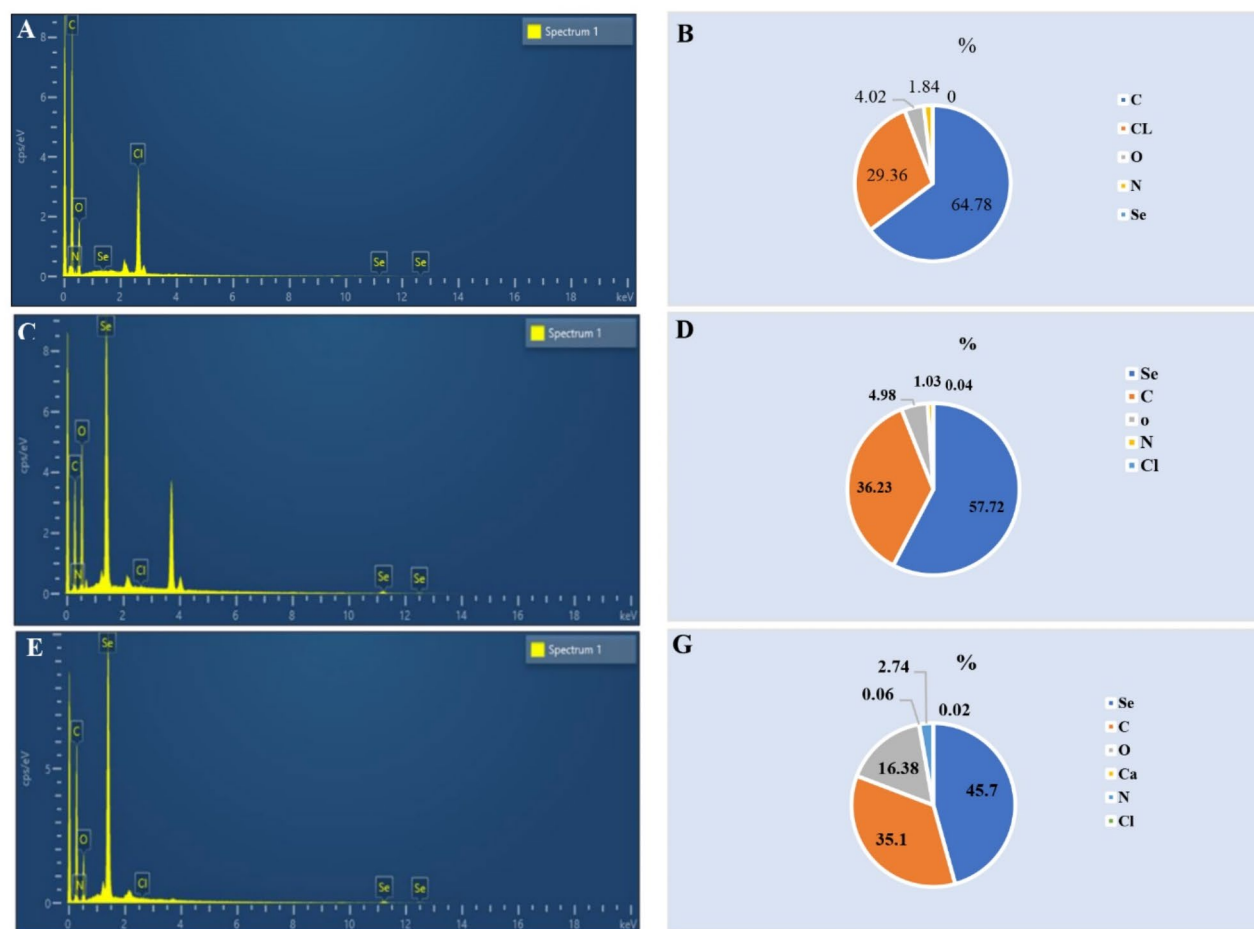


Fig. 1. EDX spectra of nanoparticles synthesized (A + B) DX spectra of NBr-NPs, (C + D) EDX spectra of Se-NPs, (E, F) EDX spectra of Br loaded on Se-NPs.

exist between the particles which prevent them from agglomerating and coming into contact with each other. The neutral particles obtained in this study can be considered intrinsically stable as they do not have any interparticulate molecular interactions, either attractive or repulsive. A zeta-potential study was performed to indicate the stability and surface charge of the created nanoparticles. The study showed the presence of a distinct peak at -31 mV for nanoparticles synthesized using the green method, indicating their good stability (supplementary Fig. 2B). The nanoparticles synthesized have capping molecules that consist mostly of negatively charged groups. These groups are responsible for the moderate stability of the nanoparticles^{23–25}. The zeta potential of Br loaded on Se-NPs shows a single net peak at -23 mV, indicating good particle stability (supplementary Fig. 2C)²⁶.

Fourier Transform Infrared spectrometer (FTIR)

In this study, The Fourier Transform Infrared spectrometer (FTIR) spectrum was used to identify the functional groups in the synthetic nanoparticles. In the FTIR spectra of Br-NPs, the following distinctive peaks can be observed: $700\text{--}1300\text{ cm}^{-1}$ (skeletal C-C vibrations), 1103.28 cm^{-1} (C-O), 1597.06 cm^{-1} and 1504.48 cm^{-1} (aromatic C=C stretching), 1504.48 cm^{-1} (skeleton vibration of aromatic C=C ring stretching), 1386.82 cm^{-1} and 1361.74 cm^{-1} (C=C stretching), 1276.88 cm^{-1} (C-O-C stretching), and $1035.77\text{--}1184.29\text{ cm}^{-1}$ (in-plane =C-H bending). Our investigation's findings were consistent with prior research^{27–29}. Functional groups present in the herbal extract, which contribute to the bonding process with Se-NPs, were identified using FTIR analysis. supplementary Fig. 3 compares the FTIR spectrum of the fruit extract with that of the manufactured Se-NPs. The O-H stretch of alcohol and phenol groups corresponded to a large vibration peak at 3430 cm^{-1} . The absorption peaks at 2977 and 2880 cm^{-1} represented the C-H stretch of the alkynes groups. Nitro compounds (N-O asymmetric stretch) were represented by the tiny band at 2320 cm^{-1} . The strong band at 1570 and 1480 cm^{-1} was related to the aromatic and alkane rings (C-C and C-H stretching). The small vibrational peaks

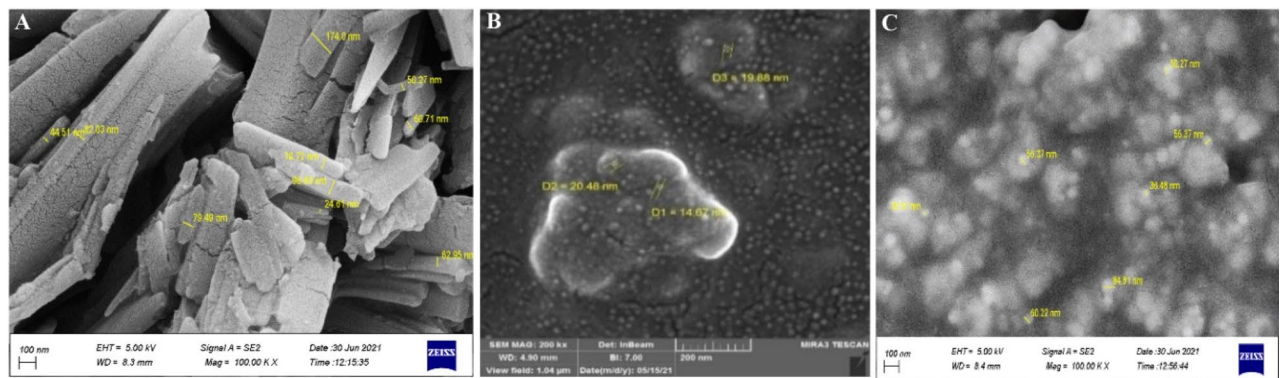


Fig. 2. FE-SEM picture of nanoparticles synthesized, (A) FE-SEM picture of synthesized Br-NPs with an average size of 75 nm. (B) FE-SEM picture of Se-NPs with an average size of 18 nm (C) FE-SEM picture of Br loaded on Se-NPs with an average size of 35 nm.

between 1376 and 1250 cm^{-1} represented the bending C-H, C-N, O-H, C-X, and C-N-C stretches, which were responsible for the alkanes, amines, and carboxylic groups. These functional groups confirm that several reducing and stabilizing agents were used in the synthesis of Se-NPs.

Determine the optimal concentration of Br, Br-NPs, Se-NPs, Br loaded on Se-NPs, and Se for sperm cryopreservation

After synthesizing nanoparticles and preparing treatments, various concentrations of Br, Br-NPs, Se-NPs, Br loaded on Se-NPs, and Se were added to fresh diluted goat semen to determine the optimum concentration. Results showed that 10 μM of Br significantly protected motility and viability rate compared to other concentrations (Fig. 3A,B). The optimal Br-NPs concentration had a significant impact on motility and viability at concentrations of 10, 1, and 0.1 μM , with 0.1 μM being selected for the next tests (Fig. 3C,D). During the process of identifying the ideal concentration, 100 μg of Se produced the best results for motility and viability rate compared to other concentrations (Fig. 3E,F). The ideal concentration of Se-NPs was found to be 1 μM , which is a hundred times lower than that of the non-nano form (sodium selenite) (Fig. 3G,H).

The study found that Br loaded on Se-NPs had a significant effect on motility and viability rate at concentrations of 10, 1, 0.1, and 0.01 μM . The concentration of 0.01 μM was ultimately chosen for the subsequent tests (Fig. 3I,J). After conducting tests, it was determined that the optimal concentrations for cryopreservation are as follows: 10 and 0.1 μM for Br and Br-NPs, 1 and 100 μg for Se-NPs and Se, and 0.01 μM for Br loaded on Se-NPs. Furthermore, the chosen concentrations for the subsequent experimental treatments were combined with the concentrations chosen for the nano and non-nano treatments.

Effect of the optimal concentrations of Br, Br-NPs, Se-NPs, Br loaded on Se-NPs, and Se on sperm parameters after thawing

The following table (Table 1) displays the effects of different treatments on goat sperm parameters after being through a freeze-thawing process. The treatments included optimal concentration of Br, Br-NPs, Se-NPs, Br-loaded Se-NPs, and Se. Results were evaluated based on sperm motility, viability, plasma membrane, and DNA integrity, as well as the levels of reactive oxygen species and lipid peroxidation.

The extender supplemented with Br-NPs (0.1 μM), Se-NPs (1 μg), and Br loaded on Se-NPs (0.01 μM) showed a significant increase in the percentage of sperm motility compared to all other treatments ($p < 0.05$). In addition, all treatments showed a significant increase in the percentage of motile spermatozoa compared to the control group ($p < 0.05$).

We used the DCFHA staining method to measure the intracellular levels of H_2O_2 and determine if ROS caused the observed damage. The proportion of sperm that was DCF positive decreased when exposed to the various treatments, with the least quantity of DCF-positive sperm being present in Br-co-Se-NPs 0.01, Br-NPs 0.1 + Se-NPs 1, and Br-NPs 0.1 ($P < 0.05$) (Fig. 4 from A to H).

To measure lipid peroxidation, we used the Bodipy staining method. The percentages of Bodipy-positive sperm significantly decreased in each treatment compared to the control group. The two treatments Br-co-Se-NPs 0.01 and Br-NPs 0.1 + Se-NPs 1 showed the lowest levels ($P < 0.05$) (Fig. 4 from I to P).

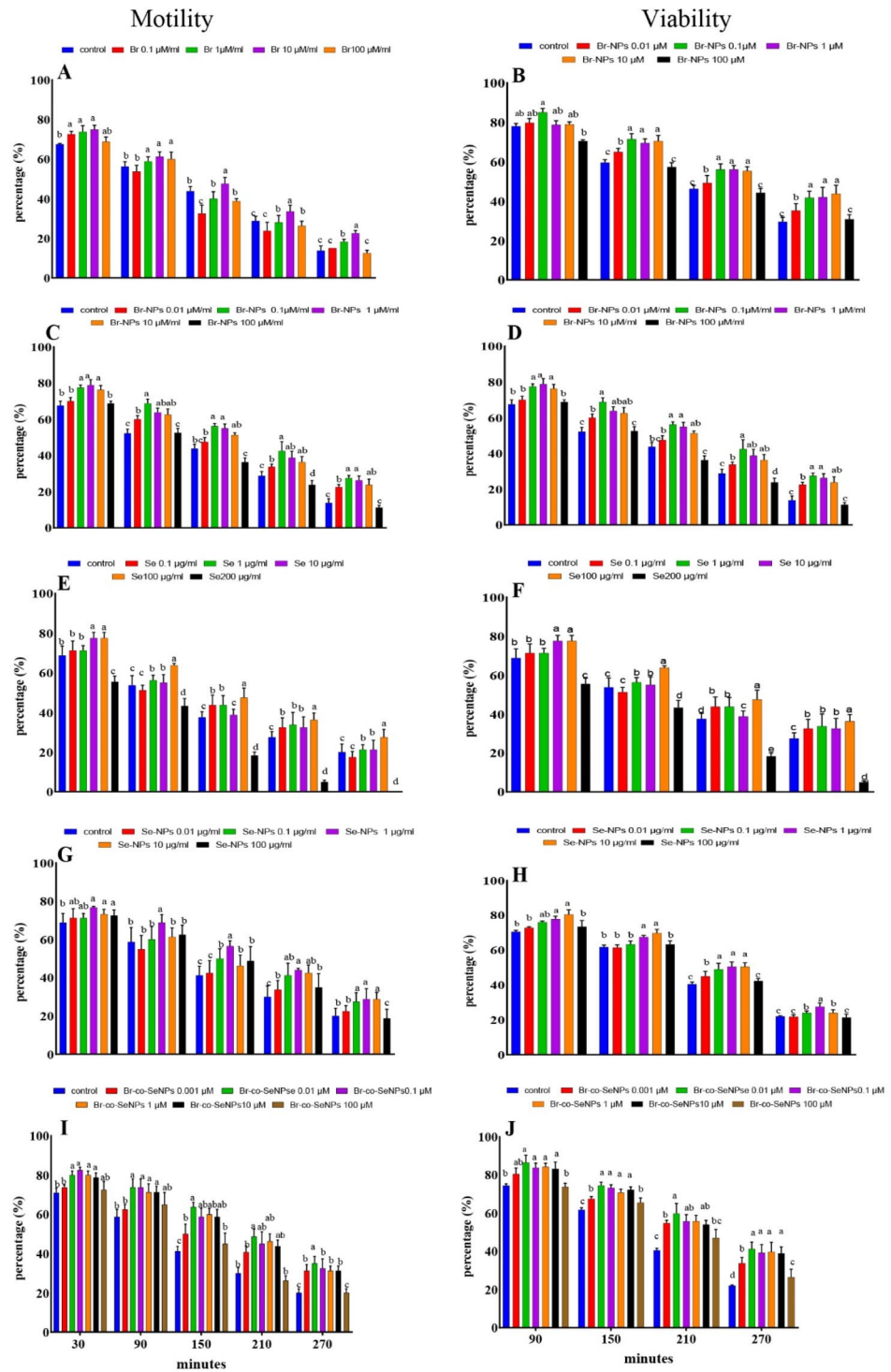


Fig. 3. Determining the optimal concentration of Br (A, B) and Br nanoparticles (C, D), Se (E, F) and Se-NPs (G, H) and Br loaded on Se NPs (I, J) by examining sperm motility and viability.

Effect of the optimal concentrations of Br, Br-NPs, Se-NPs, Br loaded on Se-NPs, and Se on in vitro embryo development

The rate of successful embryo development, including cleavage, blastocysts formation, and hatched blastocysts, significantly increased in all treatment groups compared to the control group (Table 2). However, the rate was significantly higher in the oocytes fertilized with Br -co-Se-NPs 0.01 and Br-NPs 0.1+Se-NPs1 treated spermatozoa than in all other treatment groups ($P < 0.05$). There was no significant difference between the Br-

Treatment	Motility (%)	Viability (%)	ROS	Lipid peroxidation (LPO)	Membrane integrity (%)	DNA damage (%)
Control	35 ± 2.89 ^d	41.67 ± 6.01 ^d	53.7 ± 2.6 ^a	45 ± 0.57 ^a	48.6 ± 1.85 ^d	30 ± 1.52 ^a
Br10	40 ± 2.89 ^c	58.33 ± 1.76 ^b	48 ± 0.57 ^b	39 ± 1.45 ^b	50 ± 1.52 ^c	24 ± 2.88 ^b
Br-NPs 0.1	51.6 ± 1.67 ^b	62.67 ± 1.45 ^b	25 ± 2.08 ^d	35 ± 1.15 ^b	58 ± 1.52 ^b	17 ± 2.18 ^c
Se 100	40 ± 2.89 ^c	53.67 ± 4.48 ^c	44 ± 1.45 ^b	40 ± 1.15 ^b	51 ± 1.76 ^c	17 ± 2.02 ^c
Se-NPs 1	45 ± 2.90 ^c	56.34 ± 3.28 ^b	32 ± 1.73 ^c	36 ± 0.88 ^b	58 ± 2.08 ^b	19 ± 2.08 ^c
Br10 + Se100	48.33 ± 4.41 ^b	71.33 ± 1.45 ^b	42 ± 3.78 ^b	43 ± 1.15 ^b	55 ± 3.46 ^b	23 ± 2.64 ^b
Br-NPs0.1 + Se-NPs 1	55 ± 2.90 ^a	58.66 ± 1.45 ^a	23 ± 0.57 ^d	25 ± 1.16 ^c	62 ± 1.85 ^a	14 ± 1.76 ^{cd}
Br-co-Se-NPs 0.01	58.8 ± 1.67 ^a	70.66 ± 1.42 ^a	24.4 ± 2.9 ^d	23 ± 1.73 ^c	67 ± 2.33 ^a	10 ± 1.20 ^d

Table 1. Effect of Br, Br-NPs, Se-NPs, Br loaded on Se-NPs and Se, and their best combination on sperm parameters (Mean ± SD) of goat semen following freeze-thawing. Values (Mean ± SD) within a column with different superscript letters are significantly different at $P < 0.05$. Br: berberine, Br-NPs: berberine nanoparticles, Se: sodium selenite, Se-NPs: selenium nanoparticles, Br + Se: berberine + sodium selenite, Br-NPs + Se-NPs: berberine nanoparticles + selenium nanoparticles, Br-co-Se-NPs: berberine coated on Se-NPs. Reactive oxygen species (ROS); Lipid peroxidation (LPO).

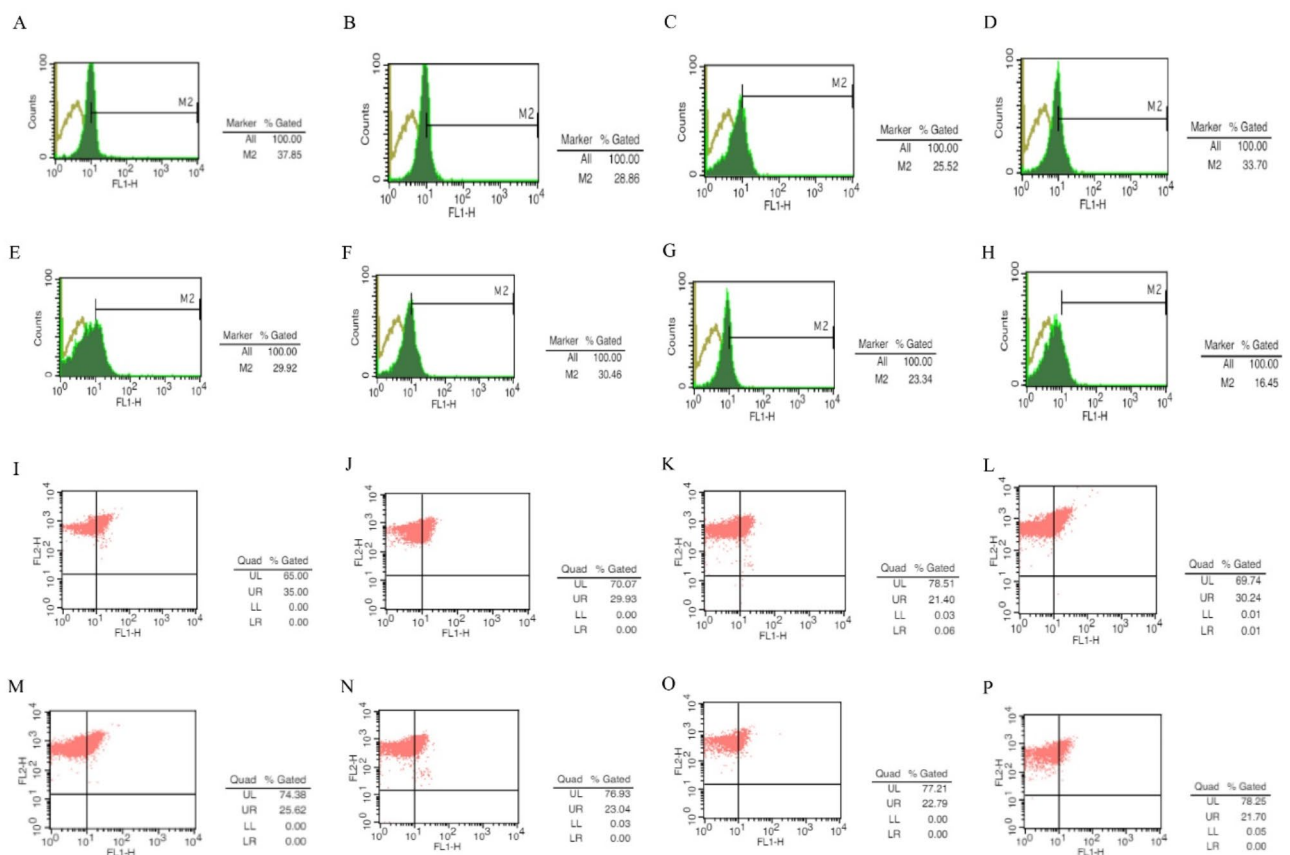


Fig. 4. Intracellular ROS levels were evaluated based on the percentage of DCF fluorescence intensity with a higher DCF considered to be an indicator of higher intracellular ROS. (A) control; (B) Br-10; (C) Br-NPs-0.1; (D) Se-100; (E) Se-NPs-1.0; (F) Br10 + Se100; (G) Br-NPs0.1 + Se-NPs1.0 and (H) Br-co-Se-NPs 0.01. Lipid peroxidation levels were evaluated based on the percentage of BODIPY 581/591 C11 fluorescence intensity with a higher BODIPY considered to be an indicator of higher lipid peroxidation. (I) control; (J) Br-10; (K) Br-NPs-0.1; (L) Se-100; (M) Se-NPs-1.0; (N) Br10 + Se100; (O) Br-NPs0.1 + Se-NPs1.0 and (P) Br-co-Se-NPs 0.01.

Embryo development			
Treatment	Cleaved	Blastocysts	Hatched Blastocyst
Control	73.45 ± 3.51 ^c	43.25 ± 6.81 ^c	33.33 ± 2.89 ^d
Br10	79.35 ± 1.73 ^{bc}	54.75 ± 7.02 ^b	40.09 ± 3.06 ^c
Br-NPs 0.1	84.67 ± 5.00 ^b	62.33 ± 4.5 ^b	50.45 ± 5.13 ^b
Se 100	81.42 ± 3.78 ^b	57.11 ± 5.03 ^b	44.67 ± 5.29 ^{bc}
Se-NPs 1	83.67 ± 4.04 ^b	59.25 ± 4.73 ^b	46.00 ± 5.29 ^{bc}
Br10 + Se100	84.67 ± 2.08 ^b	55.15 ± 4.58 ^b	42.12 ± 9.18 ^c
Br-NPs0.1 + Se-NPs 1	93.00 ± 6.50 ^a	71.94 ± 11.51 ^a	56.96 ± 4.16 ^a
Br-co-Se-NPs 0.01	94.67 ± 5.80 ^a	68.75 ± 13.03 ^a	59.73 ± 12.20 ^a

Table 2. Effect of sperms treated with br, Br-NPs, Se-NPs, Br loaded on Se-NPs and Se, and their best combination on in vitro goat embryo development. Values (Mean ± SD) within a column with different superscript letters are significantly different at $P < 0.05$. Br: berberine, Br-NPs: berberine nanoparticles, Se: sodium selenite, Se-NPs: selenium nanoparticles, Br + Se: berberine + sodium selenite, Br-NPs + Se-NPs: berberine nanoparticles + selenium nanoparticles, Br-co-Se-NPs: berberine coated on Se-NPs.

NPs 0.1 and Se-NPs groups, as well as the Br10, Se 100, and Br10 + Se100 groups in terms of blastocysts and hatched blastocyst rate, but there was a significant difference with the control group ($P < 0.05$).

Effect of the optimal concentrations of Br, Br-NPs, Se-NPs, Br loaded on Se-NPs, and Se on embryo quality

In Figs. 5 and 6, it is evident that the control group had a lower ICM number compared to the rest of the treatment groups. Among all the groups, the extender that contained Br-co-Se-NPs 0.01 and Br-NPs 0.1 + Se-NPs1 had the highest ICM number ($P < 0.05$). Similarly, the TE number in the control group was lower compared to all the other treatment groups. The extender containing Br-co-Se-NPs 0.01 and Br-NPs 0.1 + Se-NPs1 had the highest TE number among all the groups ($P < 0.05$).

Discussion

The synthesized nanoparticles were analyzed for their chemical elemental composition using EDX. In the case of Br-NPs, EDX analysis are consistent with those of previous research by Abdollahnia et al.³⁰ and Kalishwaralal et al.³¹. The peaks composed of related elements in Se-NPs and Br-co-SeNPs are also considered as a confirmation of the construction of these nanoparticles. Also, our findings regarding UV-visible absorption spectrum are consistent with the studies conducted Chung Lin et al.³² and Ozgul et al.³³. Furthermore, our results are consistent with the research published in 2020, 2018, and 2023 by Ahmed et al.³⁴, Pouri et al.³⁵ and Mohammed Ali et al.³⁶ respectively.

Based on the field emission scanning electron microscope (FE-SEM) images obtained, it can be observed that Se-NPs are almost spherical with an average diameter of approximately 18 nm. These results are consistent with previous studies, where the size of Se-NPs was found to be less than 50 nm³⁶⁻³⁸. The FE-SEM images of berberine nanoparticles reveal an average particle size of about 76 nm. This confirms the synthesis of berberine nanoparticles³⁹⁻⁴¹. The FE-SEM picture of berberine loaded on Se-NPs demonstrates an average particle size of about 35 nm and a spherical shape. This is consistent with the present study, where the average size of berberine loaded on Ag-NPs was found to be between 30 and 50 nm⁴².

Zeta potential analysis In the case of the synthesized Se-NPs, the analysis revealed a distinct peak at -41.8 mV, indicating good stability. This suggests that the capping molecules covering the surface of the Se-NPs are mainly composed of negatively charged groups, which help to maintain the particles' stability. These results are consistent with prior studies^{23,24,43}. On the other hand, the zeta potential results of the synthesized Br-NPs have a distinct peak at 0 mV (± 25 mV). A zeta potential of ± 25 mV is recommended to achieve a stable dispersion. This is because repulsive forces exist between particles, preventing them from coming into contact with each other and agglomerating.

Thus the obtained neutral particles can now be considered intrinsically stable because no interparticle molecular interactions (both attractive and repulsive) are expected from these particles. Positively charged nanoparticles are absorbed into the cell membrane at a faster rate than neutral or negatively charged particles⁴⁴. Particles with a zeta potential between -30 and 30 mV tend to clump together, which is called the isoelectric point, where the zeta potential is zero mV⁴⁵. Nanoparticles that have strong negative or positive surface charges are stable. If the zeta potential estimate is a flat ± 30 mV, then it's a general indication that the colloidal solution is highly stable⁴⁶. Recent research has shown that the peak zeta-potential for the co-assembly of berberine and tannic acid was about $+33.28$, which is not consistent with our study's results⁴⁷ but has been confirmed in Saba's study (2019)⁴⁸.

An FTIR spectrum ranging from 500 to 4000 cm^{-1} was used to examine the molecules responsible for the construction and coating of nanoparticles. The results of our study regarding Se-NPs are consistent with previous research, with minor differences possibly due to the use of different types of regenerative plant types²³. The FTIR spectrum of berberine nanoparticles in the frequency range of 500 to 4000 cm^{-1} . These results are consistent with previous studies²⁸. FTIR spectrum of Br-co-SeNPs spectrum provides information about the chemical structure

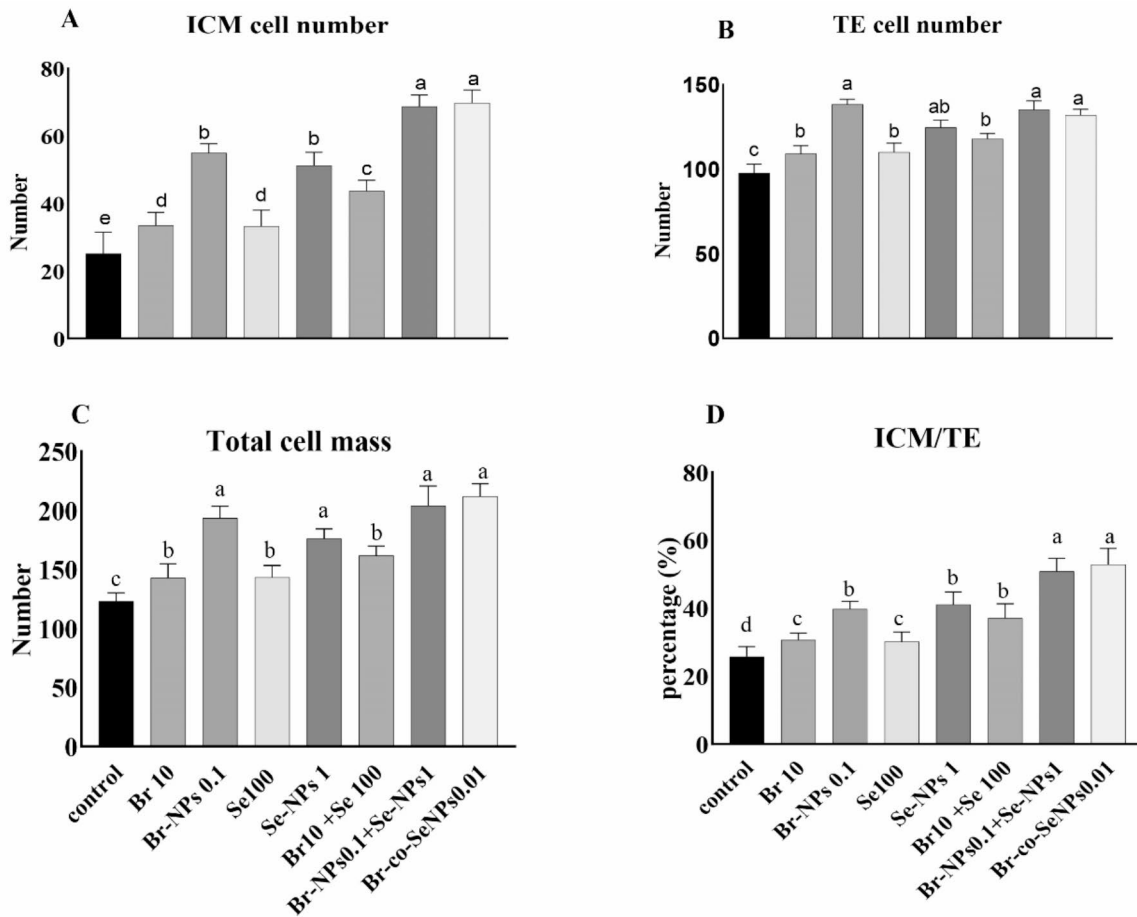


Fig. 5. Comparison between (A) inner cell mass (ICM), (B) trophoblast cells (TE), (C) total cell mass (TCM), and (D) ICM/TCN, in embryos derived from frozen/thawed goat spermatozoa with extender supplemented with Br, Br-NPs, Se, Se-NPs, Br+Se, Br-NPs+Se-NPs and Br-co-Se-NPs mean \pm standard deviation (SD), and different letters indicate significant differences ($P < 0.05$).

of the sample in the frequency range of 500 to 4000 cm. The peaks seen in this spectrum indicate the presence of various chemical bonds and functional groups that, these observations are consistent with previous studies in this regard²⁸.

It has been found that storing semen in liquid or frozen form can cause damage to the structure, biochemistry, and function of sperm. This leads to reduced motility, viability, and fertility of the sperm. Studies have shown that natural antioxidants can improve the quality of mammalian semen^{49–51}. It has not yet been determined whether Br in different forms can improve sperm quality after freeze-thawing in goat semen. In this study, we evaluated the effect of selected concentrations of Br in different forms, including Br, Br-NPs, Br loaded on Se-NPs, and Br combined with Se and Se-NPs, on cryopreservation goat semen. The study examined the qualitative parameters of sperm, including motility, viability, membrane and DNA integrity, ROS production rate, and LPO.

Sperm motility is a crucial factor in evaluating the fertility and energy status of sperm, as well as a useful test for reproductive toxicity⁵². In this study, we observed an increase in the motility, viability, and plasma membrane integrity of sperm treated with various forms of Br in vitro. Our results show that the administration of Br-10 and Br-NPs-0.1 had a dual effect on sperm motility and viability. Lower doses of Br and Br-NPs (0.1, 1, and 10 μ Mol) significantly increased motility and viability ($P < 0.05$). However, in experimental groups exposed to higher concentrations of Br-10 and Br-NPs-0.1 (100 μ Mol), motility and viability were lower compared to the control group. Our findings regarding motility and viability are in agreement with those reported by Chen et al.⁴⁹ and Tvrdá et al.⁵³. Br administered to rats with varicocele improved their motility, viability, and membrane integrity⁵⁴. In another study, it was observed that Br restored reproductive functions in diabetic rats by reducing ROS production, inhibiting apoptosis, reducing Janus kinase2 (JAK)2 activity, activating the Nuclear factor kappa B (NF κ B) pathway, and improving the disorders caused by type 2 diabetes⁵⁵. This is in line with current research findings on reducing levels of ROS and LPO, while also increasing sperm motility and viability⁵⁶.

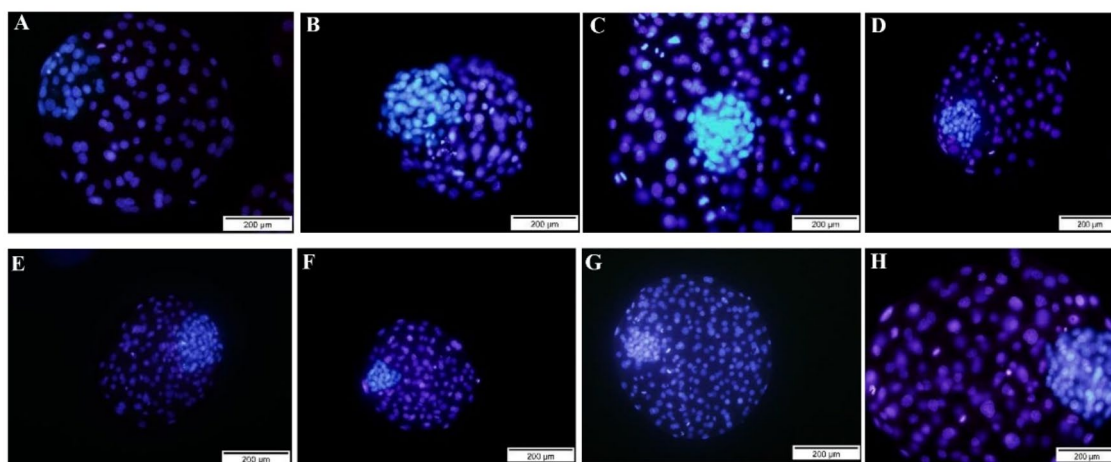


Fig. 6. Representative pictures of embryo development and differential staining of hatched blastocyst on day 8 derived from oocytes fertilized by frozen/thawed goat spermatozoa with extender supplemented with Br-10, Br-NPs-0.1, Se-100, Se-NPs-1.0, Be10 + Se100, Br-NPs-0.1 + Se-NPs-1.0 and Br-co-Se-NPs 0.01. (A) control; (B) Br-10; (C) Br-NPs-0.1; (D) Se-100; (E) Se-NPs-1.0; (F) Be10 + Se100; (G) Br-NPs0.1 + Se-NPs1.0, and (H) Br-co-Se-NPs 0.01.

Berberine has a strong effect on inhibiting lipoxygenase and xanthine oxidase. These two enzymes are important sources of reactive oxygen species (ROS) generation. This indicates that berberine hydrochloride has antioxidant properties⁵⁷. Studies have shown that berberine can prevent the oxidation of low-density lipoprotein (LDL) caused by Ca^{+2} and protect cells from dysfunction caused by oxidized LDL⁵⁸.

Zeng and colleagues demonstrated that berberine has significant effects on cell health. It increases the activity of superoxide dismutase, reduces the formation of harmful superoxide anion and malondialdehyde (MDA), and inhibits the damaging effects of H_2O_2 ⁵⁹. This is achieved through increased cell viability, nitric oxide (NO) production, and superoxide dismutase activation, while reducing the release of lactic acid dehydrogenase and MDA⁶⁰.

In this research, it was found that the treatment of Br-co-Se-NPs 0.01 and Br-NPs0.1 + Se-NPs1 during the freezing process can significantly improve the quality of goat sperm. This indicates that Se-NPs are a very effective carrier for Br delivery. The results of Yin et al.⁶¹ are also consistent with this research. Their study investigated the effect of Se as an oral nano-carrier of Br on hyperglycemia and anti-diabetic effects.

The results of this study showed that the problem of very low bioavailability of berberine can be solved with the nanobiotechnology method⁶².

Both Se and Se-NPs have been used to improve semen quality in different animal species³⁶. Similar to our study, several studies have shown that Se-NPs supplementation at a concentration of 1 mg/mL Se-NPs demonstrated the best motility and viability in sperm^{19,63}. In our experiment, a study showed that Se-NPs, compared to Se, have a significant effect on the quality of mouse sperm⁶⁴. However, the study of Hawkes et al.⁶⁵ found a positive effect of Se on human sperm at 200 mg/mL, which did not agree with our results. This may be due to the difference between the animal species tested.

Selenium is an essential component of selenoproteins such as glutathione peroxidase and thioredoxin reductase, which play vital roles in antioxidant protection and maintaining male fertility¹⁹. It is also a part of the glutathione enzyme found in the head and middle part of sperm, protecting them from oxidative damage⁶⁶. Additionally, selenium is involved in regulating the capacitation process and the acrosome reaction, both of which are crucial for sperm fertility. These processes require precise, timely, and regular performance⁶⁷.

The study found that the combined treatment of Br10 and Se100 improved motility and viability more than the control group. The results were also better than treatments with Br and Se alone, likely due to the synergistic effects of these two substances⁵⁴. The research added the tested treatments to the cryopreservation extender, which improved the structure of the plasma membrane of the sperm after the process, preserving its motility and viability. The exposure of sperm to extracellular ROS leads to the loss of membrane integrity, which is directly related to the reduction of cell viability and function⁴⁹. The study's findings regarding the integrity of the plasma membrane for Se-NPs at a concentration of 1 mg/ml were consistent with the research of Natiq et al.⁶⁸.

ROS, are harmful by-products that can result from cellular metabolism or exposure to certain substances known as xenobiotics. These by-products can cause oxidative stress in sensitive cells, which can be particularly damaging to sperm due to their high content of PUFAs, especially docosahexaenoic acid (DHA)⁶⁹. To investigate the potential role of ROS in causing damage to sperm, we assessed intracellular H_2O_2 levels using a staining method called 2',7'-Dichlorofluorescein diacetate (DCFHA). We found that the percentage of positive DCF sperm was significantly lower in all treatments compared to the control group. Furthermore, the percentage of

positive DCF sperm exposed to Br-NPs0.1 + Se-NPs1 and Br-co-Se-NPs0.01 was significantly lower than that of the control group and other treatments. These two treatments had the lowest level of positive DCF among all treatments, as well as the control group ($p < 0.05$). It is believed that disruption of the mitochondrial electron transport system can lead to excessive production of ROS, which can then cause oxidative damage when released into the extracellular space.

Br has been found to have a protective effect on mammalian cells by maintaining cellular communication channels, which helps to prevent apoptosis or necrosis. This effect is most likely due to its ability to restore the balance between complexes I, II, and IV⁵⁰. In another study, it was discovered that cow sperm exposed to Br at concentrations of 1, 10, and 50 μM showed the lowest levels of ROS production over 24 h, in comparison to higher concentrations of 100 and 200 μM . These results are consistent with previous findings⁴⁹.

The study evaluated lipid peroxidation through pie staining and confirmed the potential antioxidant capabilities of Br by assessing LPO in sperm. In the case of mammalian sperm, the suppression of LPO has been successfully achieved through the administration of antioxidants that can stop lipid peroxidation or counteract oxygen toxicity⁴⁹. Natural antioxidants have been shown to improve the quality of stored mammalian semen in several in vitro studies^{50,51,64}. The study conducted by Eva Tvrdá et al. also showed a positive effect of Br in reducing LPO, which was confirmed by the results of positive Bodipy sperm that showed the same pattern as the percentage of positive DCF ($P < 0.05$)⁴⁹.

A study has shown that Se and Se-NPs have a decreasing effect on LPO in rat sperm. Se-NPs were found to have a more significant effect on sperm quality compared to s Se⁷⁰. Another study evaluated the quality of ram semen after thawing and found that the addition of Se-NPs to a seminal fluid extender reduced lipid peroxidation while increasing sperm viability and motility⁶³. Acridine orange (AO) staining was used to evaluate any breaks in the two strands of sperm DNA, identifying sperm with broken DNA⁷¹. All treatments significantly reduced the percentage of sperm with DNA damage compared to the control group. Sperm chromatin condensation protects sperm DNA content against ROS-induced damage. Sperm cells are very sensitive to lipid peroxidation caused by ROS due to the presence of high levels of unsaturated fatty acids in their membrane structure⁷².

Our result revealed that Br had a significant positive effect on sperm chromatin condensation. This is consistent with the findings of Hassni et al.⁷³ who observed similar results in rats with varicocele. Najarian et al. (2018) also confirmed the results of our research. In our study, all treatments showed a significant decrease in sperm with damaged DNA compared to the control group. However, there was no significant difference between the Br10 and Br10 + Se100 groups, although these groups did show a significant difference compared to the Br-NPs0.1, Se100, Se-NPs1, and Br-NPs0.1 + Se-NPs1 groups ($P < 0.05$). Sperm DNA damage was significantly improved in the Br-co-Se-NPs0.01 groups compared to all other groups in the AO test ($P < 0.05$). In a similar study, Najarian et al.⁵⁴ observed that Br improved sperm DNA integrity, motility, and viability⁵⁴. Jingyu et al.⁵⁵ investigated the protective effect of Br on reproductive performance and spermatogenesis in diabetic rats through inhibition of the ROS/JAK2/NF κ B pathway and confirmed its efficacy. In another study, Hosni et al.⁷³ investigated the effect of Br on sperm parameters in varicocele patients and observed a significant improvement in the quantitative and qualitative parameters of mouse sperm.

The present study evaluated the effect of different cryopreservation treatments on the fertility ability of goat sperm and the potential development of blastocysts. Our findings indicate that the tested treatments had a positive impact on in vitro fertilization parameters and improved the developmental competence of goat oocytes. Specifically, spermatozoa treated with Br-co-Se-NPs 0.01 and Br-NPs0.1 + Se-NPs 1 showed increased fertilization ability and subsequent embryo development compared to the control group and other treatments. Additionally, the nano-groups and non-nano groups respectively showed significant differences compared to the control group. In summary, the treatments used in this study were able to positively affect the quality of in vitro fertilization, either by increasing the quality of sperm or maintaining its initial quality and fertility.

It has been suggested that the outcomes of In vitro fertilization (IVF) for cryopreservation are a reliable representation of sperm quality investigations. This is because the reduced fertilization ability of spermatozoa in IVF embryo production is likely due to a decline in motility, viability, plasma membrane integrity, and an increase in the formation of ROS and LPO of sperm⁷⁴. In 2013, a study was carried out on women with polycystic ovaries to investigate the effect of Br and metformin on this disease. The results indicated that these two substances improved the condition of patients with polycystic ovaries and increased the fertility rate. It has also been reported that higher conception rates are observed in IVF⁷⁵.

Conclusion

The study conducted has demonstrated the effects of Br in various forms, including macromolecule Br, Br-NPs, Br loaded on Se-NPs, combination with Se, as well as the effect of Se and green synthesized Se-NPs on goat sperm cryopreservation. It has also examined the in vitro fertility of these sperms and subsequent in vitro goat embryo development. The results of the study show that all of these treatments have positive effects on the sperms' motility, viability, and membrane integrity, and reduce the quantity of ROS, LPO, and DNA damage. Additionally, these modifications helped sperm's capacity for in vitro fertilization to rise. In particular, Br loaded on Se-NPs at a concentration of 0.01 μM in goat semen diluent has been found to have positive effects on sperm performance and in vitro fertility of sperm kept in frozen conditions. This is because it improves the motility, viability, and integrity of the plasma membrane, and reduces ROS, LPO, and damaged DNA. The antioxidant properties of these compounds and their status as drug-carrying nanoparticles are likely connected to this improvement. These discoveries might aid in the creation of new methods for shielding animal or human sperm from environmental stressors like cryopreservation.

In our study, we found that Berberine in various nano and carrier-loaded forms has protective effects on goat sperm fertility by reducing reactive oxygen species (ROS). However, it's important to note that our study has some limitations. We focused solely on frozen sperm and did not investigate non-frozen sperm, oocytes, and

the culture medium for oocyte growth and maturation. To address these limitations, we plan to conduct future studies to confirm the effects of this bioactive substance. Additionally, further research on the mechanisms and signaling pathways involved in the effects of different forms of nanoparticles on the protection of sperm, oocytes, and embryos is necessary.

Materials and methods

Media and reagents

All chemicals and media were obtained from Sigma Aldrich Chemical Co. (St. Louis, MO) and Gibco (Grand Island, NY), respectively, unless stated. The Royan Institute Committee approved the experimental designs and the protocol conformed to the guidelines of the Nutrient Requirements of Laboratory Animals (NRC, 2007) and Ethics Committee of Isfahan University of Technology, Isfahan, Iran (license no. 66445 National Institute for Medical Research Development). Animals were housed in standard cages under standardized laboratory conditions.

Preparation of the extract

The fruits of *Berberis vulgaris* bought from herbal shop were washed thoroughly with tap water and distilled water to remove contamination. They were then dried in the shade at room temperature for a week. After that, the dried fruits were powdered and 20 g of the powder was mixed with 200 milliliters of deionized water. The mixture was heated to 80 °C using a heater-stirrer for 30 min. The solution was then centrifuged and the supernatant was separated and filtered through Whatman's paper. The extract was obtained, stored in the refrigerator, and used the next day.

Green synthesis of Se-NPS

Depicts the preparation of Se-NPs through a green synthesis approach using the fruit extract of *Berberis vulgaris*. To prepare Se-NPs, a 0.1 M aqueous Se solution was added drop-wise to 50 mL of distilled water while constantly stirring at room temperature. The resulting solution was then mixed with 50 mL of fruit extract and stirred continuously for 24 h at 25 °C. Finally, the brick-colored powder containing Se-NPs was obtained.

Synthesis of Br nanoparticles

Br-NPs were prepared using the APSP method. In this method, a solvent (ethanol) was used to create a saturated solution of Br. This solution was then rapidly injected into a certain volume of deionized water (which acted as an anti-solvent) at a fixed flow rate of 1 mL/min. The injection was done with the help of a syringe and under mechanical stirring (3000 rpm). After stirring, the resulting mixture, which was in the form of a turbid/opaque suspension, was quickly evaporated in a vacuum using a rotary evaporator to obtain nano-sized drug particles²⁸.

Conjugation of Br on Se-NPs (Br-co-SeNPs)

Green synthetic Se-NPs were dissolved in ethanol at a concentration of 1 mg/mL along with Br. The resulting mixture was stirred at room temperature for 24 h and then centrifuged at 7000 rpm for 20 min to extract the Br-Se-NPs. The supernatant from the centrifugation was analyzed by a UV-visible spectrophotometer to confirm the effectiveness of the conjugation process. The unconjugated drug was identified by its absorbance at 250 nm and was subtracted from the total quantity of the added medication to determine the conjugation efficiency. The conjugation efficiency was calculated using the formula⁷⁶:

$$\text{Conjugation efficiency} = \frac{[(\text{Total Drug} - \text{Unconjugated Drug}) / \text{Total Drug}]}{1} \quad (1)$$

A reliable, simple, and reproducible method was developed to estimate drug concentrations in unknown samples by comparing them to standard samples of known concentrations. A calibration curve was created to determine the concentration of Br in methanol solutions by plotting Br concentrations against absorbance (max 250 nm). The Beer-Lambert law was used to calculate the drug concentration in methanol as (0.85–3.78 µg/mL). Line equations and graphs were created based on linearly reverting concentrations and absorbances. The standard curve for Br was displayed, with a relevant coefficient value of 0.944, which demonstrates that the drug complies with the Beer-Lambert rule in the concentration range of 0.1 to 0.8 µg/mL.

Characteristics of the synthesized nanoparticles

Various techniques were employed to investigate the synthesized nanoparticles. Morphological and elemental analyses of Se-NPs, Br-NPs, and Br loaded on Se-NPs (Br-co-Se-NPs) were carried out using Energy-dispersive X-ray spectroscopy (EDX) with field emission scanning electron microscopes (FE-SEM). Dry powder samples were sprayed onto carbon tape and coated with gold for the FE-SEM analysis. After the reaction, 1 mL of the purified sample was taken and sonicated at 1790 g for 15 min to prepare for ultraviolet-visible spectroscopy (UV-vis) examination. The UV-Vis spectrum was measured in the 200–800 nm wavelength range. Fourier transform infrared (FTIR) spectra were recorded in the 4000–400 cm⁻¹ region.

The electrophoretic mobility of nanoparticles in a U-type tube at 25 °C was measured using a zeta-sizer (Horiba-SZ-100-Z model) to determine the zeta-potential. FE-SEM images were also analyzed in Image J 1.48v software (National Institute of Health, USA) to determine the size of the nanoparticles.

Animals and semen collection

The study used semen samples from five adult goats, aged 2 to 3 years. The goats' ejaculates were collected twice per week for two months using an artificial vagina, and then immediately transferred to a laboratory under appropriate conditions. There, the samples were analyzed for sperm quality using a microscope. The Royan

Institute Committee approved the experimental designs and the protocol conformed to the guidelines of the Nutrient Requirements of Laboratory Animals (NRC, 2007) and Ethics Committee of Isfahan University of Technology, Isfahan, Iran (license no. 66445 National Institute for Medical Research Development). Animals were housed in standard cages under standardized laboratory conditions.

Semen extender and semen processing

The Andromed extender was used as the base extender. The volume of ejaculate was measured in a conical tube which was graduated at 0.1 mL intervals. To determine the ejaculate concentration, a hemocytometer was used. The semen parameters for the samples ranged from 0.75 to 2 mL in volume, sperm concentration of $\geq 3 \times 10^9$ spermatozoa/mL, sperm motility of $\geq 80\%$, and frequencies of total morphological abnormalities of $\leq 10\%$ ⁷⁷.

Experimental design

In experiment 1, the objective was to determine the potential effective concentration of Br in different forms. Br nanoparticles (Br-NPs: 0.01, 0.1, 1, 10, and 100 μM), Se (Se: 0.1, 1, 10, 100, and 200 $\mu\text{g}/\text{mL}$), Se-NPs (0.1, 1, 10, and 100 $\mu\text{g}/\text{mL}$), and Br loaded on Se-NPs (Br-co-Se-NPs: 0.001, 0.01, 0.1, 1, 10, and 100 μM) were tested at concentrations. The samples were incubated for 30, 90, 150, 210, and 270 min with 250×10^6 spermatozoa/mL in an Andromed extender at a temperature of 38.5°C and 5% CO_2 . The motility and viability were assessed visually and with a nigrosin–eosin staining assay at each time point.

Experiment 2 was conducted to assess whether biologically produced nanoparticles could enhance the quality of goat spermatozoa. For this experiment, goat sperm was collected using a synthetic vagina. Samples from five adult goats were combined for cryopreservation. The diluted semen samples were cooled gradually at 4°C for a few hours before being filled into 0.25 mL French straws. The straws were then placed 4 cm above liquid nitrogen (LN2) for 12 min before being submerged in LN2 and kept until the time came to measure the parameters of the sperm. After collection and evaluation, the pooled semen was divided into 8 aliquots. Each aliquot was extended with different substances, including no additives (control), Br 10 μM (Br10), Br-nanoparticles 0.1 μM (Br-NPs0.1), Se 100 μg (Se100) and selenium-nanoparticles 1 μg (Se-NPs 1). Additionally, Br loaded on selenium nanoparticles 0.01 μM (Br-co-Se-NPs) and combined concentrations of Br and selenium nanoparticles (Br-NPs0.1 μM + Se-NPs1 μg) and Br and selenium salt (Br10 μM + Se 100 μg) were used. After thawing, the evaluated parameters included sperm motility, viability, lipid peroxidation, total ROS, membrane, and DNA integrity. These were determined at the best concentrations from experiment 1 synthesized nanoparticle treatment groups.

Post-thaw semen evaluation

Sperm motility

Approximately 10 μl of the sperm suspension was placed on a warmed microscope slide and viewed at a magnification of 400x (using an Olympus CX31 microscope; Japan) to measure the spermatozoa motility. By separating immotile from motile spermatozoa in at least ten different microscopic fields, the motility of the sperm was evaluated. Finally, the following equation was used to assess sperm motility⁷⁸:

$$\text{Motility (\%)} = \left[\frac{\text{motile sperm}}{\text{motile} + \text{non-motile sperm}} \right]$$

The percentage of live and dead sperm

Using nigrosin–eosin staining, the sample's live sperm content was quantified as a percentage. To determine the viability of the sperm, one drop of freshly diluted or thawed sperm was mixed with two drops of 1% aqueous eosin. Then, two drops of 10% aqueous nigrosin were added to this mixture to create two thin smears for each sample. At least 200 sperm cells were examined using bright-field microscopy (1000x; Olympus CX31, Japan). Sperm heads that appeared white or light pink were considered viable, while those that appeared red or dark pink were considered non-viable.

Evaluation of sperm plasma membrane integrity

The Hypo-Osmotic Swelling Test (HOST) is a method used to assess the functional integrity of the sperm plasma membrane based on coiled and swollen tails. During the procedure, 30 μL of semen is incubated at 37°C for 60 min with 300 μL of a 100 mOsm hypo-osmotic solution. After incubation, 0.2 mL of the mixture is placed on a warm slide using a cover slip. 400 sperms are examined using bright-field microscopy at 400x magnification. Sperms with coiled tails are considered to have an intact membrane⁷⁹.

AO staining

AO is a fluorescent stain used to identify sperm DNA damage and maintain chromatin integrity in sperm nuclei. To prepare the samples, air-dried smears were fixed with Carnoy's fixative (3:1 mixture of methanol and acetic acid) at 4°C for two hours. The slides were then removed from the fixative and allowed to dry briefly before being stained with newly prepared AO (1 mg/mL) at room temperature for 10 min. Finally, the slides were cleaned in distilled water and examined using an Olympus BX51 fluorescence microscope on the same day. At least 200 spermatozoa from each preparation were examined at a 1000x magnification. When attached to native double-strand DNA (ds-DNA), AO emits green fluorescence; when bound to fully denatured single-strand DNA (ss-DNA), AO emits red fluorescence. A change in red-high cells provides a measurement of sperm DNA fragmentation. Thus, we determined the distribution of spermatozoa that fluoresced greenly and redly⁸⁰.

Assessment of reactive oxygen species (ROS)

The amount of intracellular H_2O_2 in the sperm was measured by using H2DCFDA staining. H2DCFDA is a dye that penetrates cells and binds to hydrophobic areas of cells. Cellular esterases break the acetate moiety, releasing an impermeable, non-fluorescent 2',7'-dichlorodihydrofluorescein (H2DCF). Intracellular H_2O_2 oxidizes H2DCF into dichlorofluorescein (DCF), which binds to DNA and produces fluorescence at 530 nm in response to 488 nm illuminations. The 2×10^6 sperm/mL in PBS that had been combined with H2DCFDA (1 μ M) and incubated at 37 °C for 20 min on the experimentation day were analyzed by a FACSCalibur flow cytometer⁷⁸.

Assessment of lipid peroxidation

BODIPY 581/591 C11 was used to measure lipid peroxidation. A suspension of 2×10^6 /mL spermatozoa was exposed to 5 μ M BODIPY 581/591 for 30 min at 37 °C. The sperm solution was then washed to remove any unbound probe before being analyzed using a FACSCalibur flow cytometer. An argon laser (488 nm) was used to excite the sample. Red fluorescence was measured using an FL3 long-pass filter (>670 nm), while green fluorescence was detected using an FL1 bandpass (BP) filter at 530/30. The analysis of 10,000 sperm-specific events was performed⁸¹.

In vitro production of caprine embryos

Oocytes collection and in vitro maturation (IVM)

Goat ovaries were obtained from two nearby slaughterhouses in Khomeini Shahr and Fasaran. Upon arrival at the embryology lab, the surrounding tissues were removed and the ovaries were stored in normal saline supplemented with penicillin/streptomycin⁸². The ovaries were then cleaned and cumulus-oocyte complexes (COCs) were extracted from follicles with a diameter of 2–6 mm using a disposable 21-gauge needle attached to a vacuum pump. Aspiration media consisting of tissue culture medium 199 (TCM199; HTCM199), 10% fetal bovine serum (FBS), and heparin (10 μ l/mL) were used. Only grade I and II oocytes were selected for in vitro maturation (IVM), and the aspirated media was transferred to a 10-cm culture dish⁸³.

To summarize, immature COCs of grades I and II were washed using H-TCM199 + 10% FBS before being randomly placed in groups of 10 in 50 μ l droplets in a predetermined maturation medium. The maturation medium contained TCM-199 tissue culture medium, 10% FBS, 1 μ g/mL estradiol 17- β , 0.01 UI/mL LH, 0.01 UI/mL FSH, 0.1 mM cysteamine, 10 ng/mL epidermal growth factor (EGF), and 100 ng/mL insulin-like growth factor (IGF)-1. The COCs were then cultured for 20 h at 38.5 °C, 5% CO_2 , and maximum humidity.

IVF and in vitro culture (IVC)

Two straws containing frozen spermatozoa from a single treatment were thawed and combined for insemination. The motile spermatozoa were separated using centrifugation with a two-layered gradient of 40% and 80% Pure Sperm (Nidacon; Gothenburg, Sweden) for 15 min at room temperature. The resulting pellet was washed using Tyrode's albumin lactate pyruvate medium. The matured COCs were also washed in a fertilization medium before insemination. For IVF, 10 mature oocytes were placed in a 50 μ l drop of fertilization medium (Fert-TALP). The oocytes were then incubated for 22 h at 38.5 °C under 5% CO_2 in humidified air, covered with mineral oil, along with 2×10^6 spermatozoa as the final concentration.

After vortexing for three minutes in 1 mL of H-TCM, the cumulus cells were removed from the presumed zygotes. Six zygotes were then transferred into 20 μ l drops of a culture medium consisting of synthetic oviduct fluid (SOF) supplemented with 8 mg/mL bovine serum albumin (BSA). The embryos were cultured in modified SOF (mSOF: SOF + FBS (10%) and glucose (1.5 mM)) for an additional 4–5 days at 38.5 °C, 5% O_2 , and 5% CO_2 under mineral oil starting on day 3 (day 0 = day of insemination) to allow them to reach the blastocyst phase. On days 3, 5, and 7 following insemination, the cleavage, blastocyst, and hatching rates in each group were assessed⁸⁴.

Differential staining

The blastocyst's quality was determined by differential staining. Briefly, the blastocysts were washed in H-TCM supplemented with 5 mg/mL BSA as a base medium. Then, the blastocysts were located in the base medium + 0.5% Triton X-100 for 20 s. Next, the fixed blastocysts were exposed to 30 mg/mL propidium iodide in the base medium for 20 s. In the last step, the blastocysts were washed and stained with ten μ g/mL of Hoechst in ethanol for 15 min at 4 °C. The blastocysts were mounted and observed by a fluorescent microscope (Olympus BX51). Inner cell mass (ICM) and trophoctoderm (TE) cells become visible as blue and red under UV light, respectively.

Statistical analysis

The data analysis was performed using SPSS20 software and either the Independent Samples T-test or the OneWay ANOVA procedure, based on the number of treatment groups tested. Tukey's test was utilized, with a significance threshold set at less than 0.05.

Data availability

"Data is provided within the manuscript or supplementary information files".

Received: 1 June 2024; Accepted: 8 October 2024

Published online: 15 October 2024

References

- Vishwanath, R. Artificial insemination: The state of the art. *Theriogenology* **59**, 571–584 (2003).
- Fiser, P. & Fairfull, R. The effects of rapid cooling (cold shock) of ram semen, photoperiod, and egg yolk in diluents on the survival of spermatozoa before and after freezing. *Cryobiology* **23**, 518–524 (1986).
- Li, P. et al. Evaluating the impacts of osmotic and oxidative stress on common carp (*Cyprinus carpio*, L.) sperm caused by cryopreservation techniques. *Biol. Reprod.* **83**, 852–858 (2010).
- Tvrđá, E., Massanyi, P. & Lukáč, N. *Spermatozoa-Facts and Perspectives* (IntechOpen, 2017).
- Sahibzada, M. U. K. et al. Berberine nanoparticles with enhanced in vitro bioavailability: Characterization and antimicrobial activity. *Drug Des. Dev. Ther.* **12**, 303 (2018).
- Mullauer, F. B. et al. Betulinic acid delivered in liposomes reduces growth of human lung and colon cancers in mice without causing systemic toxicity. *Anticancer Drugs* **22**, 223–233 (2011).
- Battu, S. K. et al. Physicochemical characterization of berberine chloride: a perspective in the development of a solution dosage form for oral delivery. *Aaps PharmSciTech.* **11**, 1466–1475 (2010).
- Zhang, S.-W., Zhou, J., Gober, H.-J., Leung, W. T. & Wang, L. Effect and mechanism of berberine against polycystic ovary syndrome. *Biomed. Pharmacother.* **138**, 111468 (2021).
- Zuo, F., Nakamura, N., Akao, T. & Hattori, M. Pharmacokinetics of berberine and its main metabolites in conventional and pseudo germ-free rats determined by liquid chromatography/ion trap mass spectrometry. *Drug Metab. Dispos.* **34**, 2064–2072 (2006).
- Feungang, J. M. et al. Treatment of boar sperm with nanoparticles for improved fertility. *Theriogenology* **137**, 75–81 (2019).
- Falchi, L. et al. Effect of exposure to CeO₂ nanoparticles on ram spermatozoa during storage at 4 °C for 96 hours. *Reprod. Biol. Endocrinol.* **16**, 1–10 (2018).
- Shahin, M. A., Khalil, W. A., Saadeldin, I. M., Swelum, A. A.-A. & El-Hairy, M. A. Comparison between the effects of adding vitamins, trace elements, and nanoparticles to shotor extender on the cryopreservation of dromedary camel epididymal spermatozoa. *Animals* **10**, 78 (2020).
- Ismail, A. A., Abdel-Khalek, A., Khalil, W. & El-Hairy, M. Influence of adding green synthesized gold nanoparticles to tris-extender on sperm characteristics of cryopreserved goat semen. *J. Anim. Poult. Product.* **11**, 39–45 (2020).
- Buazar, F. et al. Facile one-pot phytosynthesis of magnetic nanoparticles using potato extract and their catalytic activity. *Starch-Stärke* **68**, 796–804 (2016).
- Soltani, L., Samereh, S. & Mohammadi, T. Effects of different concentrations of zinc-oxide nanoparticles on the quality of ram Cauda epididymal spermatozoa during storage at 4 °C. *Reprod. Domestic Anim.* **57**(8), 864–875 (2022).
- Harshiny, M., Matheswaran, M., Arthanareeswaran, G., Kumaran, S. & Rajasree, S. Enhancement of antibacterial properties of silver nanoparticles–ceftriaxone conjugate through *Mukia maderaspatana* leaf extract mediated synthesis. *Ecotoxicol. Environ. Saf.* **121**, 135–141 (2015).
- Maidin, M. S., Adanan, N., Aminudin, M. & Tawang, A. In vitro supplements improves motility and progressive score of spermatozoa in jermasia goats. *APCBEE Procedia* **8**, 329–333 (2014).
- Dorostkar, K., Alavi-Shoushtari, S. M. & Mokarizadeh, A. *Veterinary Research Forum*. (Faculty of Veterinary Medicine Urmia University).
- Khalil, W. A., El-Hairy, M. A., Zeidan, A. E. & Hassan, M. A. Impact of selenium nano-particles in semen extender on bull sperm quality after cryopreservation. *Theriogenology* **126**, 121–127 (2019).
- Shi, L.-G. et al. Effect of elemental nano-selenium on semen quality, glutathione peroxidase activity, and testis ultrastructure in male Boer goats. *Anim. Reprod. Sci.* **118**, 248–254 (2010).
- Talebi, E., Ghasemi, F. & Haghigat Jahromi, M. Effect of Selenium nanoparticles antioxidant on sperm parameters in mature and adult rats. *J. Fasa Univ. Med. Sci.* **4**, 111–119 (2014).
- Safa, S., Moghaddam, G., Jozani, R. J., Kia, H. D. & Janmohammadi, H. Effect of vitamin E and selenium nanoparticles on post-thaw variables and oxidative status of rooster semen. *Anim. Reprod. Sci.* **174**, 100–106 (2016).
- Citrarasu, V. et al. Green synthesis of selenium nanoparticles mediated from *Ceropegia bulbosa* Roxb extract and its cytotoxicity, antimicrobial, mosquitocidal and photocatalytic activities. *Sci. Rep.* **11**, 1032 (2021).
- Raahati, Z., Bakhshi, B. & Najjar-Peerayeh, S. Selenium nanoparticles induce potent protective immune responses against *Vibrio cholerae* WC vaccine in a mouse model. *J. Immunol. Res.* **2020**, 1–12 (2020).
- Guisbiers, G. et al. Inhibition of *E. coli* and *S. aureus* with selenium nanoparticles synthesized by pulsed laser ablation in deionized water. *Int. J. Nanomed.* **11**, 3731 (2016).
- Chandrasekar, N., Kumar, K., balasubramnian, K. S., karunamurthy, K. & Varadharajan, R. Facile synthesis of iron oxide, iron-cobalt and zero valent iron nanoparticles and evaluation of their anti microbial activity, free radicle scavenging activity and antioxidant assay. *Dig. J. Nanomater. Biostruct.* **8** (2013).
- Tran, T. V. A. et al. Preparation of berberine chloride nanoparticles by ball milling method. *VNU J. Sci. Med. Pharm. Sci.* **38** (2022).
- Sahibzada, M. U. K. et al. Berberine nanoparticles with enhanced in vitro bioavailability: Characterization and antimicrobial activity. *Drug Des. Dev. Therapy*, 303–312 (2018).
- Pandey, S. et al. Biogenic gold nanoparticles as foillars to fire berberine hydrochloride using folic acid as molecular road map. *Mater. Sci. Eng. C33*, 3716–3722 (2013).
- Abdollahnia, M., Makhdomi, A., Mashreghi, M. & Eshghi, H. Exploring the potentials of halophilic prokaryotes from a solar saltern for synthesizing nanoparticles: The case of silver and selenium. *PLoS One* **15**, e0229886 (2020).
- Kalishwaralal, K., Jeyabharathi, S., Sundar, K. & Muthukumar, A. Comparative analysis of cardiovascular effects of selenium nanoparticles and sodium selenite in zebrafish embryos. *Artif. Cells Nanomed. Biotechnol.* **44**, 990–996 (2016).
- Yu-Chung, L. et al. Spectral analysis of nanodiamond-berberine complex interaction with living cells for nanoparticle mediated drug delivery. *J. Biomed. Photon. Eng.* **3**, 10305 (2017).
- Çetinkol, Ö. P. & Hud, N. V. Molecular recognition of poly (A) by small ligands: An alternative method of analysis reveals nonmolar, cooperative and shape-selective binding. *Nucleic Acids Res.* **37**, 611–621 (2009).
- Ahmed, F. et al. Development of selenium nanoparticle based agriculture sensor for heavy metal toxicity detection. *Agriculture* **10**, 610 (2020).
- Pouri, S., Motamedi, H., Honary, S. & Kazeminezhad, I. Biological synthesis of selenium nanoparticles and evaluation of their bioavailability. *Braz. Arch. Biol. Technol.* **60** (2018).
- Mohammed Ali, I. A., AL-Ahmed, H. I. & Ben Ahmed, A. Evaluation of green synthesis (*Withania somnifera*) of selenium nanoparticles to reduce sperm DNA fragmentation diabetic mice induced with streptozotocin. *Appl. Sci.* **13**, 728 (2023).
- Safaei, M. et al. Optimization of green synthesis of selenium nanoparticles and evaluation of their antifungal activity against oral *Candida albicans* infection. *Adv. Mater. Sci. Eng.* **2022**, 1–8 (2022).
- Kalishwaralal, K., Jeyabharathi, S., Sundar, K. & Muthukumar, A. A novel one-pot green synthesis of selenium nanoparticles and evaluation of its toxicity in zebrafish embryos. *Artif. Cells Nanomed. Biotechnol.* **44**, 471–477 (2016).
- Khan, I., Saeed, K. & Khan, I. Nanoparticles: Properties, applications and toxicities. *Arab. J. Chem.* **12**, 908–931 (2019).
- Laurent, S. et al. Magnetic iron oxide nanoparticles: Synthesis, stabilization, vectorization, physicochemical characterizations, and biological applications. *Chem. Rev.* **108**, 2064–2110 (2008).
- Jia, J., Zhang, K., Zhou, X., Zhou, D. & Ge, F. Precise dissolution control and bioavailability evaluation for insoluble drug berberine via a polymeric particle prepared using supercritical CO₂. *Polymers* **10**, 1198 (2018).

42. Wu, Y. et al. Ameliorative effect of berberine coated bio-active nanoparticles in acetaminophen induced hepato-renal damage in diabetic rats. *J. Photochem. Photobiol. B Biol.* **189**, 250–257 (2018).
43. Guisbiers, G. et al. Inhibition of *E. coli* and *S. aureus* with selenium nanoparticles synthesized by pulsed laser ablation in deionized water. *Int. J. Nanomed.* **11**, 3731–3736 (2016).
44. Wang, Z., Wu, J., Zhou, Q., Wang, Y. & Chen, T. Berberine nanosuspension enhances hypoglycemic efficacy on streptozotocin induced diabetic C57BL/6 mice. *Evid.-Based Complement. Altern. Med.* **2015**, 1–5 (2015).
45. Marsalek, R. Particle size and zeta potential of ZnO. *APCBEE Procedia* **9**, 13–17 (2014).
46. Bhattacharjee, S. DLS and zeta potential—what they are and what they are not?. *J. Control. Release* **235**, 337–351 (2016).
47. Zheng, T. et al. Fabrication of Co-assembly from berberine and tannic acid for multidrug-resistant bacteria infection treatment. *Pharmaceutics* **15**, 1782 (2023).
48. Al-Obaidy, S. S., Greenway, G. M. & Paunov, V. N. Dual-functionalised shellac nanocarriers give a super-boost of the antimicrobial action of berberine. *Nanoscale Adv.* **1**, 858–872 (2019).
49. Tvrdá, E., Greifová, H., Ivanič, P. & Lukáč, N. In vitro effects of berberine on the vitality and oxidative profile of bovine spermatozoa. *Int. J. Anim. Vet. Sci.* **13**, 244–249 (2019).
50. Tvrdá, E. et al. The effect of curcumin on cryopreserved bovine semen. *Int. J. Anim. Vet. Sci.* **10**, 707–711 (2016).
51. Amidi, F., Pazhohan, A., Shabani Nashtaei, M., Khodarahmian, M. & Nekoonam, S. The role of antioxidants in sperm freezing: A review. *Cell Tissue Bank.* **17**, 745–756 (2016).
52. Ugur, M. R. et al. Advances in cryopreservation of bull sperm. *Front. Vet. Sci.* **6**, 268 (2019).
53. Chen, L., Wang, T. & Liu, J. Effect of berberine on human sperm parameters in vitro. *Transl. Androl Urol.* **5**, AB229 (2016).
54. Najaran, H. et al. The protective effect of coenzyme Q10 and berberine on sperm parameters, with and without varicocelectomy in rats with surgically induced varicoceles. *Comp. Clin. Pathol.* **28**, 479–485 (2019).
55. Song, J. et al. Protective effect of Berberine on reproductive function and spermatogenesis in diabetic rats via inhibition of ROS/JAK2/NFκB pathway. *Andrology* **8**, 793–806 (2020).
56. Zhao, Q. et al. Cuscuta chinensis flavonoids reducing oxidative stress of the improve sperm damage in bisphenol A exposed mice offspring. *Ecotoxicol. Environ. Saf.* **255**, 114831 (2023).
57. Shen, L. & Ji, H.-F. The mechanisms of ROS-photogeneration by berberine, a natural isoquinoline alkaloid. *J. Photochem. Photobiol. B Biol.* **99**, 154–156 (2010).
58. Zhang, X.-D., Ren, H.-M. & Liu, L. Effects of different dose berberine on hemodynamic parameters and [Ca²⁺]_i of cardiac myocytes of diastolic heart failure rat model. *Zhongguo Zhong yao za zhi Zhongguo Zhongyao Zazhi China Journal of Chinese Materia Medica* **33**, 818–821 (2008).
59. Liu, W. et al. Berberine inhibits aldose reductase and oxidative stress in rat mesangial cells cultured under high glucose. *Arch. Biochem Biophys.* **475**, 128–134 (2008).
60. Tan, Y., Tang, Q., Hu, B. R. & Xiang, J. Z. Antioxidant properties of berberine on cultured rabbit corpus cavernosum smooth muscle cells injured by hydrogen peroxide 1. *Acta Pharmacol. Sinica* **28**, 1914–1918 (2007).
61. Yin, J., Hou, Y., Yin, Y. & Song, X. Selenium-coated nanostructured lipid carriers used for oral delivery of berberine to accomplish a synergic hypoglycemic effect. *Int. J. Nanomed.* **12**, 8671–8680 (2017).
62. Younis, F. A. et al. Preparation, physicochemical characterization, and bioactivity evaluation of berberine-entrapped albumin nanoparticles. *Sci. Rep.* **12**, 17431 (2022).
63. Nateq, S., Moghaddam, G., Aljani, S. & Behnam, M. The effects of different levels of Nano selenium on the quality of frozen-thawed sperm in ram. *J. Appl. Anim. Res.* **48**, 434–439 (2020).
64. Bucak, M. N. et al. Effects of antioxidants on post-thawed bovine sperm and oxidative stress parameters: Antioxidants protect DNA integrity against cryodamage. *Cryobiology* **61**, 248–253 (2010).
65. Hawkes, W. C. & Turek, P. J. Effects of dietary selenium on sperm motility in healthy men. *J. Androl.* **22**, 764–772 (2001).
66. Ebisch, I., Pierik, F., De Jong, F., Thomas, C. & Steegers-Theunissen, R. Does folic acid and zinc sulphate intervention affect endocrine parameters and sperm characteristics in men?. *Int. J. Androl.* **29**, 339–345 (2006).
67. Aitken, R., Harkiss, D., Knox, W., Paterson, M. & Irvine, D. A novel signal transduction cascade in capacitating human spermatozoa characterised by a redox-regulated, cAMP-mediated induction of tyrosine phosphorylation. *J. Cell Sci.* **111**, 645–656 (1998).
68. Li, S. et al. Glutathione and selenium nanoparticles have a synergistic protective effect during cryopreservation of bull semen. *Front. Vet. Sci.* **10**, 1093274 (2023).
69. Aitken, R. J., Wingate, J. K., De Iulius, G. N., Koppers, A. J. & McLaughlin, E. A. Cis-unsaturated fatty acids stimulate reactive oxygen species generation and lipid peroxidation in human spermatozoa. *J. Clin. Endocrinol. Metab.* **91**, 4154–4163 (2006).
70. Khalaf, A., Ahmed, W., Moselhy, W., Abdel-Halim, B. & Ibrahim, M. Protective effects of selenium and nano-selenium on bisphenol-induced reproductive toxicity in male rats. *Hum. Exp. Toxicol.* **38**, 398–408 (2019).
71. Evenson, D. P. Sperm chromatin structure assay (SCSA*) for fertility assessment. *Curr. Protoc.* **2**, e508 (2022).
72. Moshaghion, S.-M., Malekinejad, H., Razi, M. & Shafie-Irannejad, V. Silymarin protects from varicocele-induced damages in testis and improves sperm quality: Evidence for E2f1 involvement. *Syst. Biol. Reprod. Med.* **59**, 270–280 (2013).
73. Hassani-Bafrani, H., Najaran, H., Razi, M. & Rashtbari, H. Berberine ameliorates experimental varicocele-induced damages at testis and sperm levels; evidences for oxidative stress and inflammation. *Andrologia* **51**, e13179 (2019).
74. Gomes, M. et al. Effect of in vitro exposure to lead chloride on semen quality and sperm DNA fragmentation. *Zygote* **23**, 384–393 (2015).
75. An, Y. et al. The use of berberine for women with polycystic ovary syndrome undergoing IVF treatment. *Clin. Endocrinol.* **80**, 425–431 (2014).
76. Greenwald, R. B., Choe, Y. H., McGuire, J. & Conover, C. D. Effective drug delivery by PEGylated drug conjugates. *Adv. Drug Deliv. Rev.* **55**, 217–250 (2003).
77. Sharafi, M. et al. In vitro comparison of soybean lecithin based-extender with commercially available extender for ram semen cryopreservation. (2009).
78. Naderi, N., Souri, M., Nasr Esfahani, M. H., Hajian, M. & Tanhaei Vash, N. Ferulago angulata extract ameliorates epididymal sperm toxicity in mice induced by lead and diazinon. *Andrology* **8**, 706–718 (2020).
79. Bucak, M. N. et al. The influence of trehalose, taurine, cysteamine and hyaluronan on ram semen: Microscopic and oxidative stress parameters after freeze–thawing process. *Theriogenology* **67**, 1060–1067 (2007).
80. Agdam, H. R., Razi, M., Amniattalab, A., Malekinejad, H. & Molavi, M. Co-administration of vitamin E and testosterone attenuates the atrazine-induced toxic effects on sperm quality and testes in rats. *Cell J.* **19**, 292 (2017).
81. Aitken, R. J., Wingate, J. K., De Iulius, G. N. & McLaughlin, E. A. Analysis of lipid peroxidation in human spermatozoa using BODIPY C11. *MHR Basic Sci. Reprod. Med.* **13**, 203–211 (2007).
82. Sadeghi, M. et al. Developmental competence of IVF and SCNT goat embryos is improved by inhibition of canonical WNT signaling. *Plos one* **18**, e0281331 (2023).
83. Davachi, N. D., Kohram, H. & Zainoalini, S. Cumulus cell layers as a critical factor in meiotic competence and cumulus expansion of ovine oocytes. *Small Rumin. Res.* **102**, 37–42 (2012).
84. Naderi, N., Hajian, M., Souri, M., Esfahani, M. H. N. & Vash, N. T. Ferulago angulata extract improves the quality of buck spermatozoa post-thaw and counteracts the harmful effects of diazinon and lead. *Cryobiology* **98**, 17–24 (2021).

Acknowledgements

The authors would like to express their gratitude to Royan Institute for their full support.

Author contributions

M.P., M.H., L.S. and N.T.V. carried out all the experimental procedures. A.H.M., M.H.N., and M.H. were involved in design and supervision of the project. M.P., A.H.M., and M.H. were involved in the preparation of the manuscript. All authors reviewed the manuscript.

Declarations

Competing interests

The authors declare no competing interests.

Additional information

Supplementary Information The online version contains supplementary material available at <https://doi.org/10.1038/s41598-024-75792-5>.

Correspondence and requests for materials should be addressed to A.H.M. or M.H.

Reprints and permissions information is available at www.nature.com/reprints.

Publisher's note Springer Nature remains neutral with regard to jurisdictional claims in published maps and institutional affiliations.

Open Access This article is licensed under a Creative Commons Attribution-NonCommercial-NoDerivatives 4.0 International License, which permits any non-commercial use, sharing, distribution and reproduction in any medium or format, as long as you give appropriate credit to the original author(s) and the source, provide a link to the Creative Commons licence, and indicate if you modified the licensed material. You do not have permission under this licence to share adapted material derived from this article or parts of it. The images or other third party material in this article are included in the article's Creative Commons licence, unless indicated otherwise in a credit line to the material. If material is not included in the article's Creative Commons licence and your intended use is not permitted by statutory regulation or exceeds the permitted use, you will need to obtain permission directly from the copyright holder. To view a copy of this licence, visit <http://creativecommons.org/licenses/by-nc-nd/4.0/>.

© The Author(s) 2024